ISGSR 2022

Bayesian Updating of Slope Reliability under Rainfall Infiltration with Field Observations

Shui-Hua Jiang[1], Xian Liu[2] and Iason Papaioannou[3]

[1]School of Infrastructure Engineering, Nanchang University, Nanchang, Jiangxi 330031, China.
E-mail: sjiangaa@ncu.edu.cn
[2]School of Civil Engineering, Sun Yat-Sen University, Zhuhai 519082, China.
E-mail: liux597@mail2.sysu.edu.cn
[3]Engineering Risk Analysis Group, Technische Universität München. Arcisstraße 21, 80333 Munich,
German.
E-mail: iason.papaioannou@tum.de

Abstract: Reliability analyses of rainfall-induced slope stability often ignore the effect of field observations, including the observation that the slope remains stable under its natural condition and/or that the slope survives under a past extreme rainfall event. In this paper, the BUS (Bayesian Updating with Structural reliability methods) method, originally proposed by Straub and Papaioannou (2015), is employed to conduct Bayesian inverse analyses of spatially varying hydraulic and shear strength parameters with the field observations. Stationary lognormal random field models are established to depict the spatial distribution features of the hydraulic and shear strength parameters. An infinite slope model is taken as an example to evaluate the probability of slope failure under a target rainfall event within the framework of Monte-Carlo simulation. This analysis allows incorporating the field observations to evaluate the rainfall-induced slope failure probability in spatially variable soils. The research outcomes can provide a new perspective to understand the rainfall-induced slope failure mechanism.

Keywords: slope reliability; rainfall infiltration; spatial variability; Bayesian inverse analysis; field observation.

1   Introduction

Landslide is one of the major geohazards in the world. Intense rainfall events are one of the most significant triggering factors of catastrophic landslides. Rainfall infiltration leads to an increase in water content and unit weight of the soil, which in turn reduces the shear strength and matric suction (e.g., Cho 2014; Yuan et al. 2019). The study of Christian and Baecher (2011) reported that "the estimated probabilities of slope failure under rainfall infiltration are at least an order of magnitude larger than the observed frequency of adverse performance". One possible reason for this discrepancy might be attributed to overestimation of the uncertainties arising from soil properties, in situ measurements and modeling of infiltration process (e.g., Christian and Baecher 2011; Jiang et al. 2022). To address this issue, the rainfall-induced slope failure mechanism and reliability problems considering the spatial variability of hydraulic and shear strength parameters were extensively investigated (e.g., Cho 2014; Liu et al. 2021). Another underlying reason for this difference might lie in the fact that the field observations, such as the slope remains stable under its natural condition and/or that the slope survives under a past extreme rainfall event, are often ignored in the reliability analyses of slope stability (e.g., Zhang et al. 2014). To the best of our knowledge, only Liu et al. (2021) conducted the slope reliability analysis for an existing slope at a specific site considering both the rainfall triggering mechanism and slope's performance records during previous rainfall events.

To elucidate the impacts of the field observations on the failure mechanism and reliability estimate of spatially varying slopes under rainfall infiltration, this study conducts the slope reliability analysis under a target rainfall event based on the Bayesian inverse analysis results of spatially varying hydraulic and shear strength parameters. The event that the slope survived under a past rainfall triggering event is treated as the field observation, which is used in the Bayesian inverse analysis.

2   Bayesian inverse analysis of spatially varying soil parameters

Bayesian methods can incorporate the field observations to improve the quantification of the uncertainties of soil parameters. This process is implemented through estimating the posterior distribution of soil parameters given the field observations. According to the Bayes' theorem, the posterior probability density function (PDF) of soil parameters can be calculated as (e.g., Straub and Papaioannou 2015; Jiang et al. 2018; Liu et al. 2021)

$$f_X''(\boldsymbol{x}) = aL(\boldsymbol{x})f_X'(\boldsymbol{x}) \tag{1}$$

where $f'_X(\boldsymbol{x})$ and $f''_X(\boldsymbol{x})$ are the prior and posterior PDFs of the random variables $\boldsymbol{X}$, $\boldsymbol{X} = \left(X_1, X_2, \ldots, X_n\right)^{\mathrm{T}}$, respectively, in which n is the number of random variables; $\boldsymbol{x}$ is a realization of input random vector $\boldsymbol{X}$ describing the uncertainties of soil parameters; $L(\boldsymbol{x})$ is the likelihood function, which is proportional to the probability of the observation information given $\boldsymbol{X} = \boldsymbol{x}$; a is the proportionality constant, $a = 1 / \int_{R^n} L(\boldsymbol{x}) f'_X(\boldsymbol{x}) d\boldsymbol{x}$.

To accurately model the soil spatial variability, the dimension n of $\boldsymbol{X}$ is typically large (Jiang et al. 2018). For the evaluation of $f''_X(\boldsymbol{x})$ in Eq. (1), a numerical solution is often required. In this study, the Bayesian Updating with Structural reliability (BUS) method originally proposed by Straub and Papaioannou (2015) is adopted. The BUS method transforms a Bayesian inverse problem into an equivalent structural reliability problem by defining an observation information domain Ω_X:

$$\Omega_X = \{p - cL(\boldsymbol{x}) \leq 0\} \tag{2}$$

where p is the realization of a standard uniform random variable in the interval [0, 1]; c is the likelihood multiplier, which needs to satisfy the inequality for all $\boldsymbol{x}$, $cL(\boldsymbol{x}) \leq 1.0$. Then, the subset simulation is employed to solve the equivalent structural reliability problem (e.g., Papaioannou et al. 2015; Jiang et al. 2018).

Because of the model error ε of slope stability analysis methods (e.g., limit equilibrium method, finite element method), the actual factor of safety (y) can be evaluated as (e.g., Depina et al. 2020; Liu et al. 2021)

$$y = FS(\boldsymbol{x}) + \varepsilon \tag{3}$$

where $FS(\boldsymbol{x})$ denotes the estimated factor of safety at $\boldsymbol{x}$. For convenience, the model error, ε, is modeled as a normal random variable with mean of μ_ε and standard deviation of σ_ε according to Depina et al. (2020) and Liu et al. (2021). Of course, it can also be modeled as a multiplicative lognormal random variable (e.g., van der Krogt et al. 2021). To incorporate the field observation that the slope survived under a past rainfall triggering event for estimating the posterior PDFs of soil parameters, the likelihood function $L(\boldsymbol{x})$ is established as

$$L(\boldsymbol{x}|y > 1.0) \propto P\left[\varepsilon > 1.0 - FS(\boldsymbol{x})\right] = 1 - P\left[\varepsilon < 1.0 - FS(\boldsymbol{x})\right] = 1 - \Phi\left[\frac{1.0 - FS(\boldsymbol{x}) - \mu_\varepsilon}{\sigma_\varepsilon}\right] \tag{4}$$

where $\Phi(.)$ is the standard normal cumulative distribution function (CDF). Thereafter, the posterior distribution, including the posterior statistics (means, standard deviations and coefficients of variation), of spatially variable soil parameters can be calculated using the BUS method with subset simulation. Based on these, the slope performance, including seepage, stability and reliability, under a future target rainfall triggering event can be readily evaluated.

3   Probabilistic slope seepage and stability analysis under rainfall infiltration

Rainfall-induced landslides are usually characterized by shallow failure modes that develop parallel to the slope surface. The depth of slip surface is around 1-3 m, which is much less than the slope length (e.g., Cho 2014; Zhang et al. 2014). The slope seepage and stability under rainfall infiltration are typically evaluated through an infinite slope model, as shown in Figure 1. A one-dimensional water flow model is used to simulate the vertical rainfall infiltration process on the slope. The governing equation of water flow on the slope can be described by Richards' equation, which is expressed as (Cho 2014)

$$\frac{\partial \theta}{\partial t} = \frac{\partial}{\partial z}\left[\left(\frac{\partial h}{\partial z} - \cos\alpha\right)k\right] \tag{5}$$

where θ is the volumetric water content, $\theta \in [\theta_r, \theta_s]$, in which θ_s and θ_r are the saturated and residual volumetric water contents, respectively; α is the slope angle; h is the pressure head; z is the depth of soil slice; k is the hydraulic conductivity, which is estimated from the saturated hydraulic conductivity (k_s) through a soil-water characteristic curve (SWCC). The commonly used van Genuchten-Mualem model (van Genuchten 1980) is chosen as the SWCC to simulate the relationship between the soil water content, hydraulic conductivity and the matric suction. The Hydrus-1D software is employed to perform the unsaturated seepage analysis under the rainfall infiltration. The distributions of pressure head and pore water pressure along the depth for each time step can be obtained by taking the realizations of random field of k_s as inputs in the SWCC. Then, the factor of safety of the infinite slope based on the Mohr-Coulomb failure criterion can be calculated as (Cho 2014)

$$FS = \frac{c' + [(\sigma_n - u_a) - \sigma_s]\tan\varphi'}{W \sin\alpha \cos\alpha} \tag{6}$$

where c' and φ' are the effective cohesion and friction angle, respectively; W is the total weight of soil at the depth z; σ_n is the total stress due to the self-weight of soil, $\sigma_n = \gamma_t z \cos^2 \alpha$, in which γ_t is the total unit weight of soil; u_a is the pore air pressure; σ_s is the suction stress, which can be estimated as

$$\sigma_s = \begin{cases} -S_e \psi, & u_w < 0 \\ u_w, & u_w \geq 0 \end{cases} \tag{7}$$

where S_e is the effective degree of saturation; ψ is the matric suction, $\psi = u_a - u_w$, in which u_w is the pore water pressure.
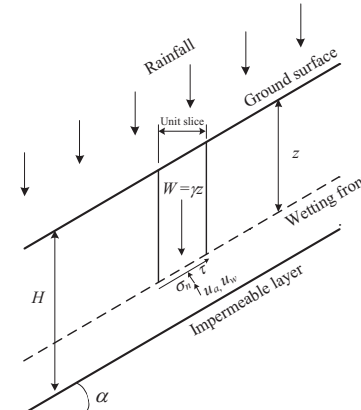
Figure 1. Infinite slope failure model.

To consider the change of soil weight due to the moisture content under the rainfall infiltration, the W of soil is estimated by integration of the unit weight γ_t in the vertical direction from the slope surface to the potential slip surface (Cho 2014). Based on these, the point-wise probability of failure (p_f) of slope for different rainfall durations t can be calculated in the framework of Monte-Carlo simulation (MCS) as follows:

$$p_f(t) = P\left[FS(\boldsymbol{x},t) + \varepsilon < 1.0\right] = \Phi\left[\frac{1.0 - FS(\boldsymbol{x},t) - \mu_\varepsilon}{\sigma_\varepsilon}\right] = \frac{1}{N}\sum_{i=1}^{N} I\left[FS(\boldsymbol{x}^i,t) + \varepsilon^i < 1.0\right] \tag{8}$$

where N is the number of MCS samples; $\boldsymbol{x}^i$ and ε^i are the i-th realization of the random fields of soil hydraulic and shear strength parameters (k_s, c' and φ') and model error, respectively; $I(.)$ is the indicator function. Note that it is assumed that the model errors at the observation and failure event are independent, in which case the model error is not learned for estimating the posterior failure probability in Eq. (8) and the information can only be used to learn the random field parameters.

4   Illustrative example

Shallow failures are commonly observed for the slope under the rainfall infiltration, thus the infinite slope model in Figure 1 that has been studied by Liu et al. (2021) is employed here to explore the effect of the field observation on slope reliability estimate. As shown in Figure 1, the infinite slope has an angle of $\alpha = 35°$ and a vertical soil thickness of $H = 2$ m. The soil layer is initially unsaturated with a uniform matric suction. The bottom of the soil layer is underlain by an impermeable layer. The values of soil physical and mechanical parameters are summarized in Table 1.

Table 1 Values of soil physical and mechanical parameters.

Soil parameters	Values	Soil parameters	Values
Saturated hydraulic conductivity k_s	2.0×10^{-6} mm/s	Initial matric suction ψ_0	10 kPa
Saturated volumetric water content θ_s	0.469	Residual volumetric water content θ_r	0.106
SWCC fitting parameter a	9.245 kPa	SWCC fitting parameter n	1.395
Effective friction angle φ'	32°	Effective cohesion c'	5 kPa
Unit weight of dry soil γ_d	16 kN/m³	Unit weight of water γ_w,	9.8 kN/m³

4.1   Bayesian inverse analyses of spatially varying soil parameters

First, deterministic seepage and stability analyses of the slope under a past rainfall event are conducted. Figure 2 shows the past rainfall event with hourly patterns and a total cumulative rainfall of around 220 mm at the slope site. It is obvious that the distribution of rainfall intensity over the time is not uniform. The Hydrus-1D software is then adopted to numerically evaluate the distribution of pore water pressure under this past rainfall event. To account for the impact of rainwater redistribution on the slope stability, a total of 240 h (10 days) is considered for analysis. Figure 3 shows the variations of the pore water pressure along the depth for different time steps. As observed from Figure 3, the matric suction is reduced to zero at the ground surface after a short duration of rainfall in Figure 2. After the rainfall finishes at the time of 18 h, the rainwater continues to infiltrate the slope and eventually reaches the impermeable layer under the rainwater redistribution. The vertical profile of pore water pressure almost keeps unchanged when the time reaches 240 h. Based on the obtained pore water pressure results, the factor of safety can be readily calculated using Eq. (6). Figure 4 presents the variation of the factor of safety with the time under the past rainfall event. It can be seen that the factor of safety also reaches convergence at the time of 240 h. This is because the rainwater has been sufficiently infiltrated and gathered at the impermeable layer.

To account for the influence of the inherent spatial variability of soil properties, the saturated hydraulic conductivity k_s, effective cohesion c' and effective friction angle φ' are modeled as stationary lognormal random fields. The slope profile is discretized into a total of 40 soil layers with a thickness of 0.05 m. Following Cho (2014) and Liu et al. (2021), k_s, c' and φ' are considered to obey lognormal distributions with means of 2.0×10^{-6} mm/s, 5 kPa and 32°, and Coefficients of Variation (COVs) of 0.6, 0.3 and 0.2, respectively. The Karhunen-Loève (KL) expansion method (Cho 2014) is utilized to generate the realizations of the random fields of k_s, c' and φ' for each soil layer. The squared exponential autocorrelation function with a vertical autocorrelation distance of 0.5 m is adopted. It is found that the random field discretization can meet the accuracy demands when the number of KL expansion terms to be retained is chosen as 5 for each random field. Then, the direct MCS with $N = 100,000$ samples is used to estimate the probability of slope failure under the past rainfall event using Eq. (8). As observed in Figure 5, the probability of slope failure increases from 5.7% to 45% under the rainwater redistribution, eventually reaches convergence at the time of 240 h.
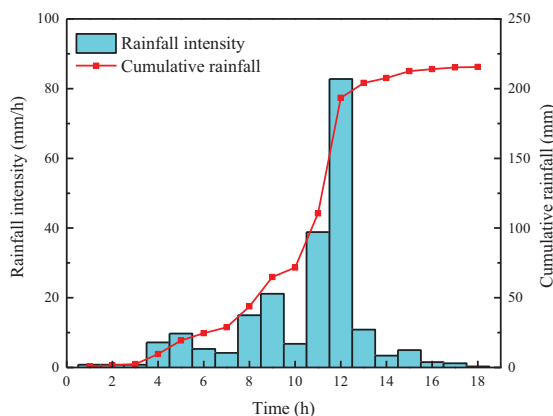

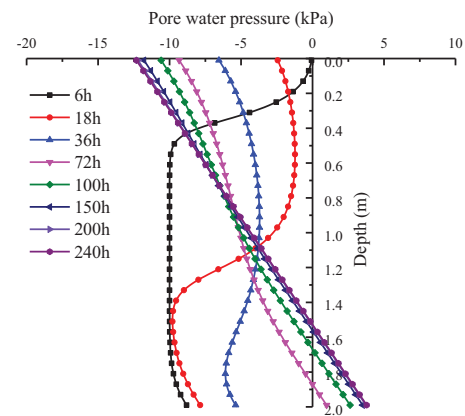**Figure 2.** A past rainfall event (adopted from Liu et al. 2021).

Figure 3. Distribution of pore water pressure under the past rainfall event.
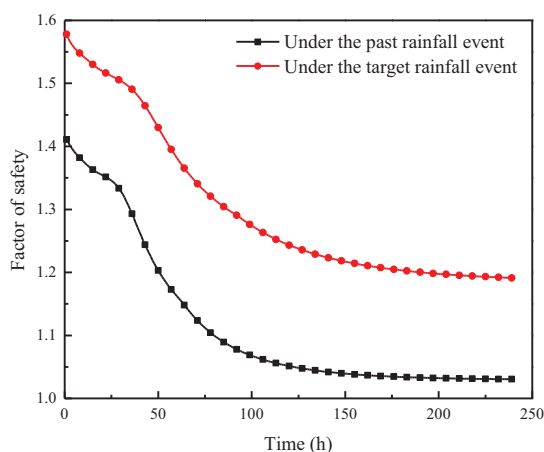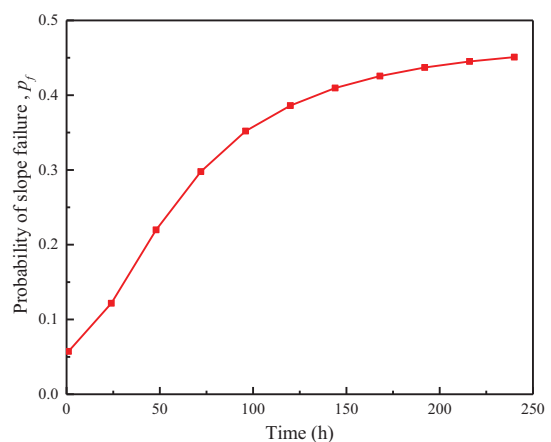

Figure 4. Variation of the factor of safety with time.

Figure 5. Variation of the probability of slope failure with time.

According to Depina et al. (2020), the model error ε in Eq. (3) is assumed to follow a normal distribution with mean $\mu_\varepsilon = 0$ and standard deviation $\sigma_\varepsilon = 0.05$. The likelihood function incorporating the field observation that the slope survived ($FS > 1.0$) under the past rainfall event in Figure 2 is established using Eq. (4). The BUS method with subset simulation is then adopted for the Bayesian inverse analyses of spatially varying soil parameters (k_s, c' and φ'). Herein, a total of 120 random variables are involved. To ensure sufficient exploration of the posterior distribution, 2,000 subset samples with a conditional probability of 0.1 for each subset level are adopted. Furthermore, 10 independent subset simulation runs are carried out, and the average calculated results across the 10 independent runs are used in the subsequent analyses. Figure 6 compares the prior and posterior PDFs and CDFs of k_s, c' and φ' at the depth of $z = 1.975$ m. It can be found from Figure 6, the variation in the probability distributions of k_s and c' is much smaller than that of φ', indicating that the φ' has a greater effect on the slope stability. Figures 7 and 8 further compare the prior and posterior means and COVs of k_s, c' and φ' along the depth, respectively. As observed from Figures 7 and 8, the posterior means and COVs of k_s, c' and φ' vary along the depth, which confirms that the stationary random fields of three soil parameters have been updated as non-stationary random fields. The posterior means of k_s along the depth are less than the corresponding prior mean, particularly close to the ground surface, while the posterior means of c' and φ' along the depth are greater than the corresponding prior means, particularly close to the impermeable layer. Moreover, as seen from Figure 8, the posterior COVs of k_s, c' and φ' along the depth are all less than the corresponding prior COVs (i.e., 0.6, 0.3, and 0.2), respectively. This implies that the Bayesian updating with the field observation effectively reduces the uncertainties and obtains more realistic statistical information of soil parameters.
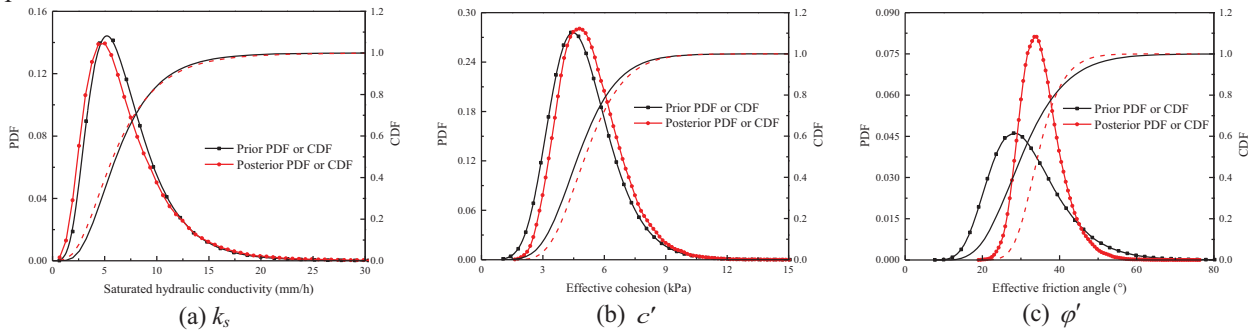

(a) k_s (b) c' (c) φ'

Figure 6. Comparison of the prior and posterior PDFs and CDFs of soil parameters ($z = 1.975$ m).

(a) k_s (b) c' (c) φ'
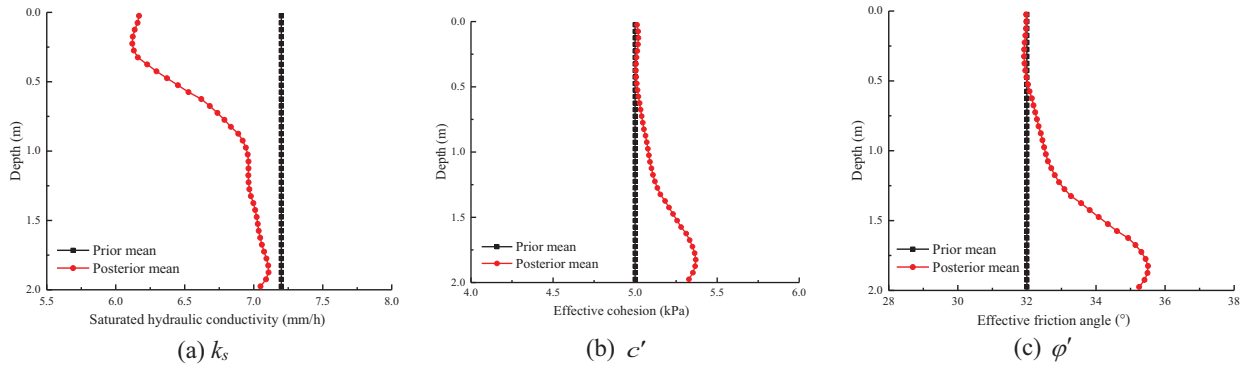
Figure 7. Comparison of the prior and posterior means of soil parameters along the depth.

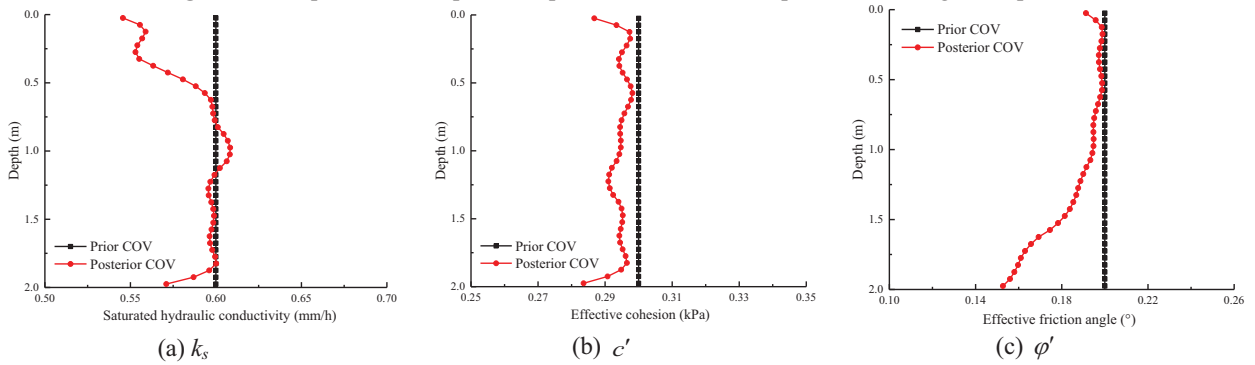(a) k_s (b) c' (c) φ'

Figure 8. Comparison of the prior and posterior COVs of soil parameters along the depth.

4.2   Reliability analysis of slope under a target rainfall event

Based on the updated statistical information of soil parameters in Section 4.1, deterministic and reliability analyses of the slope seepage and stability under a target rainfall event are carried out. Figure 9 shows the target rainfall event with duration of 18 h and a total cumulative rainfall of 241 mm. The variations of the pore water pressure along the depth for different time steps under the target rainfall event for the posterior mean of k_s are similar to those in Figure 3. The factors of safety for different time steps estimated using Eq. (6) based on the posterior means of soil parameters are also plotted in Figure 4. As seen from Figure 4, the factors of safety under the target rainfall event are larger than those under the past rainfall event. Furthermore, the posterior probability of slope failure is readily evaluated using the MCS in Eq. (8) based on the obtained 107,620 posterior samples of soil parameters (k_s, c' and φ'). Figure 10 compares the variations of the prior probability of failure and the posterior probability of failure conditional on the field observation with the time. The posterior probability of slope failure that incorporates the field observation is close to zero (1.58×10^{-4}) at the beginning of target rainfall event and increases to 14.06% at the time of 240 h. As seen from Figure 10, the probability of failure will be significantly overestimated if the field observation is ignored, especially at the beginning of target rainfall event. This aligns well with the observation that the estimated probability of slope failure is always larger than the actual observed landslide probability as indicated by Christian and Baecher (2011). Moreover, the proposed framework is efficient in the computation. The computational time taken for the Bayesian inverse analysis and the estimate of posterior probability of failure under the target rainfall event is 32.4 h and 28.7 h, respectively, on a desktop computer with an Intel (R) Core (TM) i9-9900K processor with 3.6 GHz main frequency and a RAM of 32 GB.
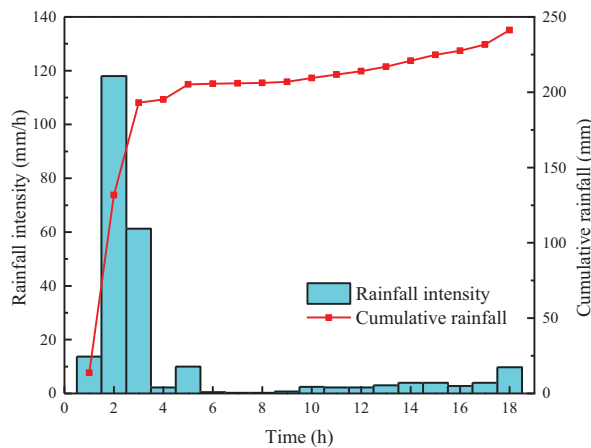

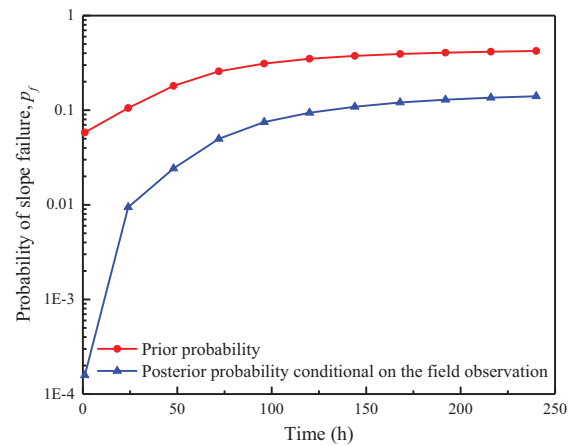**Figure 9.** A target rainfall event (adopted from Liu et al. 2021).

Figure 10. Variation of the probability of slope failure with the time.

5   Conclusions

In this paper, the influence of the field observation that the slope survived under a past rainfall triggering event on the identification of soil parameters and reliability estimate of slope stability is addressed. First, the Bayesian inverse analyses of the spatially varying hydraulic and shear strength parameters are conducted using the BUS method with subset simulation. Then, the slope reliability under a target rainfall event is evaluated based on the updated statistical information of soil parameters. For the considered infinite slope example, the effective friction angle has a greater effect on the slope stability. The probabilities of failure will be overestimated more than one order of magnitude if the field observation is ignored, especially at the beginning of the rainfall. The reason that the estimated probabilities of slope failure are usually larger than the observed frequency of adverse performance is due to overestimation of the uncertainties of soil parameters.

References

Christian, J. T. and Baecher, G. B. (2011). Unresolved problems in geotechnical risk and reliability. Geo-Risk 2011, *Risk Assessment and Management*, 50-63.
Cho S. E. (2014). Probabilistic stability analysis of rainfall-induced landslides considering spatial variability of permeability. *Engineering Geology*, 171, 11-20.

Depina, I., Oguz, E. A., and Thakur, V. (2020). Novel Bayesian framework for calibration of spatially distributed physical-based landslide prediction models. *Computers and Geotechnics*, 125, 103660.

Jiang, S.H., Papaioannou, I., and Straub, D. (2018). Bayesian updating of slope reliability in spatially variable soils with in-situ measurements. *Engineering Geology*, 239, 310-320.

Jiang, S. H., Huang, J., Griffiths, D. V., and Deng, Z. P. (2022). Advances in reliability and risk analyses of slopes in spatial variable soils: A state-of-the-art review. *Computers and Geotechnics*, 141, 104498.

Liu, X. and Wang, Y. (2021). Reliability analysis of an existing slope at a specific site considering rainfall triggering mechanism and its past performance records. *Engineering Geology*, 288, 106144.

Papaioannou, I., Betz, W., Zwirglmaier, K., and Straub, D. (2015). MCMC algorithms for subset simulation. *Probabilistic Engineering Mechanics*, 41, 89-103.

Straub, D. and Papaioannou, I. (2015). Bayesian updating with structural reliability methods. *Journal of Engineering Mechanics*, 141(3), 04014134.

van Genuchten M. T. (1980). A closed-form equation for predicting the hydraulic conductivity of unsaturated soils. *Soil Science Society of America Journal*, 44(5), 892-898.

van der Krogt, M. G., Schweckendiek, T., and Kok, M. (2021). Improving dike reliability estimates by incorporating construction survival. *Engineering Geology*, 280, 105937.

Yuan, J., Papaioannou, I., and Straub, D. (2019). Probabilistic failure analysis of infinite slopes under random rainfall processes and spatially variable soil. *Georisk*, 13(1), 20-33.

Zhang, J., Huang, H. W., Zhang, L. M., Zhu, H. H., and Shi, B. (2014). Probabilistic prediction of rainfall-induced slope failure using a mechanics-based model. *Engineering Geology*, 168, 129-140.